Published in final edited form as:
Neuron. 2008 October 9; 60(1): 111–122. doi:10.1016/j.neuron.2008.08.024.

Prostatic acid phosphatase is an ectonucleotidase and suppresses pain by generating adenosine

Mark J. Zylka[1,#,*], **Nathaniel A. Sowa**[1,#], **Bonnie Taylor-Blake**[1], **Margaret A. Twomey**[1], **Annakaisa Herrala**[2], **Vootele Voikar**[3], and **Pirkko Vihko**[2,4,*]

[1]*Department of Cell and Molecular Physiology, UNC Neuroscience Center, University of North Carolina, CB #7545, Chapel Hill, North Carolina 27599* [2]*Department of Biological and Environmental Sciences, Division of Biochemistry, P.O. Box 56, FI-00014, University of Helsinki, Finland* [3]*Neuroscience Center, P.O. Box 56, FI-00014, University of Helsinki, Finland* [4]*Biocenter Oulu and Research Center for Molecular Endocrinology, P.O. Box 5000, FI-90014, University of Oulu, Finland*

SUMMARY

Thiamine monophosphatase (TMPase, also known as Fluoride-Resistant Acid Phosphatase) is a classic histochemical marker of small-diameter dorsal root ganglia neurons. The molecular identity of TMPase is currently unknown. We found that TMPase is identical to the transmembrane isoform of Prostatic Acid Phosphatase (PAP), an enzyme with unknown molecular and physiological functions. We then found that PAP knockout mice have normal acute pain sensitivity but enhanced sensitivity in chronic inflammatory and neuropathic pain models. In gain-of-function studies, intraspinal injection of PAP protein has potent anti-nociceptive, anti-hyperalgesic and anti-allodynic effects that last longer than the opioid analgesic morphine. PAP suppresses pain by functioning as an ecto-5'-nucleotidase. Specifically, PAP dephosphorylates extracellular adenosine monophosphate (AMP) to adenosine and activates A_1-adenosine receptors in dorsal spinal cord. Our studies reveal molecular and physiological functions for PAP in purine nucleotide metabolism and nociception and suggest a novel use for PAP in the treatment of chronic pain.

INTRODUCTION

Painful and tissue-damaging stimuli are sensed by small-diameter nociceptive neurons, located in the dorsal root ganglia (DRG) and trigeminal ganglia (Woolf and Ma, 2007). For nearly fifty years, it was known that many small-diameter DRG neurons expressed a histochemically identifiable acid phosphatase (Colmant, 1959), commonly referred to as Fluoride-Resistant Acid Phosphatase (FRAP) or Thiamine Monophosphatase (TMPase) (Dodd et al., 1983;

*Co-corresponding authors, **Mark J. Zylka** Dept. of Cell & Molecular Physiology, 5109A NRB, CB #7545, 115 Mason Farm Road, University of North Carolina, Chapel Hill, NC 27599-7545, Tel: 919-966-2540, Fax: 919-966-6927, Email: zylka@med.unc.edu **Pirkko Vihko** Department of Biological and Environmental Sciences, Division of Biochemistry, P.O. Box 56, FI-00014, University of Helsinki, Finland, Tel: +358-40-5431734, Email: pirkko.vihko@helsinki.fi.
#Authors contributed equally

AUTHOR CONTRIBUTIONS: M.J.Z. empirically determined that PAP was TMPase, conceived the work, designed the experiments, supervised the project and wrote the manuscript. N.A.S. performed *in situ* hybridizations, phosphatase assays, intrathecal injections and behavioral assays. B.T-B. performed histological experiments. M.T. collected tissue for histology, performed intrathecal injections, SNI surgeries and behavioral assays. A.H. and P.V. generated and provided PAP knockout mice and tissues. V.V. and P.V. conducted preliminary behavioral experiments with PAP knockout mice. M.J.Z. and P.V. shared unpublished data to facilitate this study.

Knyihar-Csillik et al., 1986). TMPase dephosphorylates diverse substrates, including the Vitamin B_1 derivative thiamine monophosphate (TMP) and 5'-nucleotide monophosphates (Dodd et al., 1983; Sanyal and Rustioni, 1974; Silverman and Kruger, 1988a).

TMPase was intensively studied in the 1980s in an effort to determine its molecular identity and function. TMPase marks most nonpeptidergic DRG neurons, a subset of peptidergic DRG neurons and unmyelinated axon terminals in lamina II of the dorsal spinal cord (Carr et al., 1990; Dalsgaard et al., 1984; Dodd et al., 1983; Hunt and Rossi, 1985; Knyihar-Csillik et al., 1986; Nagy and Hunt, 1982; Silverman and Kruger, 1988a). Since peptidergic and nonpeptidergic neurons are generally considered to be nociceptive (Woolf and Ma, 2007), these anatomical studies suggested TMPase might function in nociception. Moreover, TMPase staining in lamina II of spinal cord is reduced or eliminated when peripheral nerves are damaged (Colmant, 1959; Csillik and Knyihar-Csillik, 1986; Shields et al., 2003; Tenser, 1985; Tenser et al., 1991). Ultimately, studies of TMPase waned when it was found that isolectin B4 (IB4) co-localized with TMPase and was an easier-to-use marker of nonpeptidergic neurons (Silverman and Kruger, 1988b; Silverman and Kruger, 1990). More importantly, the gene encoding TMPase was never identified, making it impossible to study the molecular and physiological function of TMPase in sensory neurons.

In an attempt to identify the TMPase gene, Dodd and co-workers partially purified TMPase protein from rat DRG using chromatography (Dodd et al., 1983). The partially purified rat protein was inhibited by the non-selective acid phosphatase inhibitor L(+)-tartrate and was similar in molecular weight to the secretory isoform of human prostatic acid phosphatase (PAP, also known as ACPP), the only known isoform of PAP at the time (Ostrowski and Kuciel, 1994). These biochemical experiments hinted that TMPase might be secretory PAP (Dodd et al., 1983). However, subsequent studies using anti-PAP antibodies failed to immunostain small-diameter DRG neurons and their axon terminals in lamina II (i.e. the neurons and axons that contain TMPase) (Dodd et al., 1983; Silverman and Kruger, 1988a). As summarized by Silverman and Kruger in 1988, these data made it impossible to determine if TMPase was PAP or some other enzyme.

In light of this unsolved question regarding the molecular nature of TMPase and the historical use of TMPase as a nociceptive neuron marker, we sought to definitively identify the TMPase gene and ascertain its function in nociception. Our experiments revealed that TMPase was a recently-discovered transmembrane (TM) isoform of PAP (TM-PAP) (Quintero et al., 2007) and was not the secretory isoform of PAP. This molecular identification then allowed us to use modern molecular and genetic approaches to rigorously study the function of PAP/TMPase in nociceptive circuits. Using our PAP knockout mice, we found that deletion of PAP increased thermal hyperalgesia (increased pain sensitivity) and mechanical allodynia in animal models of chronic pain. Conversely, a single intraspinal injection of PAP protein had anti-nociceptive, anti-hyperalgesic and anti-allodynic effects that lasted for up to three days, much longer than a single injection of the commonly used opioid analgesic morphine. Mechanistically, we found that PAP is an ectonucleotidase that dephosphorylates extracellular AMP to adenosine and requires A_1-adenosine receptors (A_1Rs) for anti-nociception.

PAP has been intensively studied for seventy years in the prostate cancer field (Gutman and Gutman, 1938). Despite decades of research, the molecular and physiological functions for PAP remained unknown. Our studies with pain-sensing neurons are the first to identify the *in vivo* substrate, the molecular mechanism and the physiological function for this medically-relevant protein. Moreover, we are the first to show that PAP functions in nociception. Considering that TM-PAP is expressed throughout the body (Quintero et al., 2007), PAP could regulate diverse physiological processes that are dependent on adenosine (Jacobson and Gao, 2006).

RESULTS

Prostatic acid phosphatase is TMPase in dorsal root ganglia sensory neurons

In rats, mice and humans, PAP is expressed as a secreted protein or as a type 1 transmembrane (TM) protein, with the catalytic acid phosphatase domain localized extracellularly (Figure 1A) (Quintero et al., 2007; Roiko et al., 1990; Vihko, 1979). The secretory isoform has been used as a diagnostic marker for prostate cancer for nearly seventy years whereas the TM isoform was only recently discovered (Gutman and Gutman, 1938; Quintero et al., 2007). To determine if either PAP isoform is expressed in DRG, we performed *in situ* hybridization with isoform-specific antisense riboprobes. These experiments revealed that TM-PAP was expressed in a subset of small-diameter DRG neurons (Figure 1B), while the secretory isoform was expressed at low-to-undetectable levels (Figure 1C). Importantly, TM-PAP is localized to the plasma membrane and vesicular membranes, just like TMPase (Csillik and Knyihar-Csillik, 1986; Quintero et al., 2007). We also found that PAP was expressed in human DRG using RT-PCR and intron-spanning primers (data not shown), consistent with localization of TMPase to small-diameter human DRG neurons (Silverman and Kruger, 1988a).

To directly test whether PAP had TMPase histochemical activity, we overexpressed mouse TM-PAP in HEK 293 cells, then stained these cells using TMP histochemistry. Cells transfected with TM-PAP were heavily stained when the plasma membrane was left intact (Figure 2A), indicating that TM-PAP can dephosphorylate TMP extracellularly. TMPase staining was even greater when the plasma membrane was permeabilized with detergent (Figure S1H). In contrast, control cells transfected with empty vector were not stained (Figure 2B). Two additional phosphatases [soluble acid phosphatase 1 (ACP1) and placental alkaline phosphatase] lacked TMPase activity (Figure S1).

DRG neurons express at least eight different acid phosphatase genes (M.J.Z, unpublished expression profiling studies), any one of which could be TMPase. To determine if PAP was the only enzyme in sensory neurons capable of dephosphorylating TMP, we analyzed DRG and spinal cord tissues from $PAP^{\Delta 3/\Delta 3}$ (henceforth referred to as $PAP^{-/-}$) knockout mice (Vihko et al., abstract from Proceedings of the AACR, 2005, 96th Annual Meeting, Anaheim, CA). In these mice, deletion of exon 3 causes complete loss of secretory and transmembrane PAP catalytic activity (Vihko et al., abstract from Proceedings of the AACR, 2005). Strikingly, TMP histochemical staining of DRG neurons and axon terminals in spinal cord was abolished in $PAP^{-/-}$ mice (Figure 2C–F). Absence of TMP staining in $PAP^{-/-}$ mice was not due to developmental loss of DRG neurons, as wild-type and $PAP^{-/-}$ mice had equivalent numbers of P2X3-expressing neurons relative to all $NeuN^{+}$ neurons in lumbar ganglia (43.4 ± 1.9% verses 42.4 ± 1.9% (s.e.m.); 1,500 $NeuN^{+}$ neurons counted per genotype). P2X3 is an ATP-gated ion channel that is co-localized with PAP (see below). Moreover, loss of TMPase staining in the spinal cord was not due to loss of axon terminals in the dorsal horn (Figure S2). These gain- and loss-of-function experiments conclusively prove that TMPase in small-diameter DRG neurons is the transmembrane isoform of PAP.

In addition, by combining immunofluorescence and TMP histochemistry, we observed co-localization between PAP and TMPase in DRG neurons (Figure S3A–C) and in axon terminals in lamina II of the spinal cord (Figure S3D–F). This anti-PAP antibody did not stain DRG or spinal cord sections from $PAP^{-/-}$ mice, confirming antibody specificity.

Lastly, upon finding that PAP was TMPase, we re-analyzed two published microarray data sets that measured changes in gene expression in DRG following peripheral nerve injury (Costigan et al., 2002; Davis-Taber, 2006). In both studies, PAP was one of the most heavily downregulated genes. This is consistent with the fact that TMPase histochemical activity is

greatly reduced in DRG and dorsal horn after peripheral nerve injury (Colmant, 1959; Csillik and Knyihar-Csillik, 1986; Shields et al., 2003; Tenser, 1985; Tenser et al., 1991).

PAP is primarily expressed in nonpeptidergic DRG neurons

TMPase was previously localized to nonpeptidergic DRG neurons and a small number of peptidergic neurons (Carr et al., 1990; Dalsgaard et al., 1984; Hunt and Mantyh, 2001; Nagy and Hunt, 1982; Silverman and Kruger, 1988b). To show that PAP had a similar distribution and to identify additional proteins that were co-localized with PAP, we performed double-label immunofluorescence with our anti-PAP antibody and various sensory neuron markers. Cell counts from confocal images revealed that virtually all nonpeptidergic DRG neurons, as defined by the markers IB4, *Mrgprd-EGFPf* and P2X3, co-expressed PAP (Figure 3A–I, Table S1). Moreover, PAP^+ axons terminated in lamina II of spinal cord in association with nonpeptidergic neuron markers (Figure S4A–F). In contrast, a smaller percentage (17.1%) of peptidergic $CGRP^+$ neurons (n=1364 cells counted) expressed PAP (Figure 3J–L, Table S1) and there was minimal overlap between PAP^+ and peptidergic ($CGRP^+$) axon terminals in spinal cord (Figure S4G–I). Lastly, 19.1 ± 1.3% of PAP^+ neurons expressed the capsaicin and noxious heat receptor TRPV1 (Figure 3M–O). Taken together, these confocal imaging studies revealed that PAP was preferentially expressed in nonpeptidergic, presumably nociceptive, DRG neurons.

Chronic pain-induced thermal hyperalgesia and mechanical allodynia is enhanced in PAP knockout mice

PAP was generally thought to function only in the prostate (Ostrowski and Kuciel, 1994). However, our expression data suggested that PAP might also function in nociceptive neurons. To evaluate pain-related functions for PAP, we tested age-matched wild-type C57BL/6 and $PAP^{-/-}$ male mice (backcrossed to C57BL/6 for 10 generations) using acute and chronic pain behavioral assays. We found no significant differences between genotypes using a measure of mechanical sensitivity (electronic von Frey) or several different measures of acute noxious thermal sensitivity (Table S2). In contrast, $PAP^{-/-}$ mice showed significantly greater thermal hyperalgesia and mechanical allodynia relative to wild-type mice in the Complete Freund's Adjuvant (CFA) model of chronic inflammatory pain (Figure 4A, B). In addition, $PAP^{-/-}$ mice showed significantly greater thermal hyperalgesia in the spared nerve injury (SNI) model of neuropathic pain (Figure 4C, D) (Shields et al., 2003).

PAP has potent and long-lasting anti-nociceptive properties

Since deletion of PAP enhanced sensitivity in two different models of chronic pain, we hypothesized that excess PAP should have the opposite effect and reduce pain. To test this, we took advantage of the fact that secretory PAP protein is commercially available and has the same N-terminal catalytic region as TM-PAP (Figure 1A). We injected wild-type mice intrathecally (i.t.) into the lumbar region of spinal cord with pure human (h)PAP protein (the secretory isoform). Control mice were injected i.t. with an equivalent amount of heat-denatured, and hence phosphatase-inactive, hPAP protein. In all cases, we determined that hPAP was active or inactive using a sensitive fluorometric-based phosphatase assay (see Experimental Procedures). We then measured noxious thermal and mechanical sensitivity before (baseline, BL) and after hPAP injections (Figure 5A, B). Six hours after i.t. injection of hPAP, paw withdrawal latency to a noxious thermal stimulus significantly increased relative to controls and remained elevated for three days (Figure 5A). This anti-nociceptive effect was dose-dependent (Figure S5) and required PAP catalytic activity (Figure 5A). Active hPAP did not alter mechanical sensitivity (Figure 5B) nor did it cause paralysis or sedation. This long-lasting anti-nociceptive effect was species-conserved as a single i.t. injection of bovine (b)PAP also increased thermal withdrawal latency for two days but had no effect on mechanical

sensitivity (Figure S6). Lastly, i.t. injection of an unrelated protein (bovine serum albumin) or large quantities of a different secreted phosphatase (bovine alkaline phosphatase) did not alter thermal or mechanical sensitivity (Figures S6, S7).

We next used the same behavioral assay to compare PAP anti-nociception to the commonly-used opioid analgesic morphine. We found that PAP and morphine anti-nociception were similar in magnitude following a single i.t. injection (40.8 ± 3.3% verses 62.2 ± 9.9% increase above baseline at the highest doses, respectively) but PAP anti-nociception lasted much longer than morphine (3 d verses 5 h at the highest doses, respectively. Figures S5, S8). Similarly, Grant and colleagues found that the same high dose of morphine (50 μg, i.t., single injection) lasted 4.6 ± 1.0 h in mice (Grant et al., 1995).

We next evaluated the extent to which hPAP affected hyperalgesia and allodynia in the CFA model of inflammatory pain and the SNI model of neuropathic pain. For both chronic pain assays, we used the uninjured paw as control. Strikingly, in both chronic pain models, a single i.t. injection of active hPAP was anti-hyperalgesic *and* anti-allodynic in the inflamed/injured paw (Figure 5C–F). As before, a single injection was effective for several days and phosphatase activity was required for these anti-nociceptive effects.

Since $PAP^{-/-}$ mice showed enhanced hyperalgesia and allodynia in the CFA inflammatory pain model (Figure 4A, B), we next tested whether hPAP could rescue these enhanced thermal and mechanical phenotypes in $PAP^{-/-}$ mice. We found that i.t. injection of hPAP increased thermal withdrawal latency in the control paw of $PAP^{-/-}$ mice to the same extent as wild-type mice (Figure 6A, blue lines). This demonstrated that $PAP^{-/-}$ mice were competent to respond to acute increases in PAP activity. Strikingly, injection of hPAP rescued the thermal and mechanical inflammatory pain phenotype in the inflamed paw of $PAP^{-/-}$ mice (Figure 6A, B, compare red lines where PAP was injected to black lines where inactive PAP was injected). Importantly, these data also suggest that localized, spinal injection of hPAP can rescue the behavioral deficit caused by deletion of PAP throughout the animal.

PAP suppresses pain by generating adenosine, a known analgesic in mammals

The anti-nociceptive effects of PAP require catalytic activity. This suggested PAP might generate, via dephosphorylation, a molecule that regulates nociceptive neurotransmission in the spinal cord. PAP and TMPase can dephosphorylate many different substrates (Dziembor-Gryszkiewicz et al., 1978; Sanyal and Rustioni, 1974; Silverman and Kruger, 1988b; Vihko, 1978). We focused on AMP because dephosphorylation of AMP produces adenosine—a molecule that inhibits nociceptive neurotransmission in spinal cord slices and has well-studied analgesic properties in mammals (Li and Perl, 1994; Liu and Salter, 2005; Post, 1984; Sawynok, 2006).

At the time we began our studies, there was no direct proof that PAP or TMPase could generate adenosine from AMP. Instead, production of adenosine was inferred by measuring production of inorganic phosphate (Vihko, 1978). To directly test whether PAP could generate adenosine from AMP and other adenine nucleotides, we incubated PAP with 1 mM AMP, ADP or ATP at pH 7.0 for 4 h. We then detected adenine nucleotides and adenosine using high performance liquid chromatography (HPLC) and UV absorbance (Lazarowski et al., 2004). These studies revealed that PAP can rapidly dephosphorylate AMP and, to a much lesser extent ADP, to adenosine (Figure 7A, B). Importantly, no unexpected peaks were seen in the chromatograms (Figure 7B, data not shown), ruling out the possibility that PAP had additional hydrolytic activities towards nucleotides.

Next, we tested the extent to which PAP could dephosphorylate extracellular AMP in HEK 293 cells, DRG neurons and spinal cord using AMP enzyme histochemistry. HEK 293 cells

transfected with TM-PAP were heavily stained whereas control cells were not (Figure 7C, D), highlighting that TM-PAP dephosphorylates extracellular AMP and hence has ecto-5'-nucleotidase activity. In addition, small-diameter DRG neurons from wild-type mice were intensely stained while large-diameter neurons had weak granular cytoplasmic staining. In contrast, only weak granular staining was present in DRG neurons from *PAP*$^{-/-}$ mice (Figure 7E, F). These data indicate that PAP is the predominant ecto-5'-nucleotidase on the soma of small-diameter neurons. Lastly, AMP histochemical staining of axon terminals in lamina II was reduced in *PAP*$^{-/-}$ relative to wild-type mice, but was not eliminated (Figure 7G, H). This indicates that PAP is one of perhaps many enzymes in spinal cord with the ability to dephosphorylate AMP to adenosine.

Adenosine mediates anti-nociception through G_i-coupled A_1-adenosine receptors (A_1Rs) (Lee and Yaksh, 1996; Sawynok, 2006). To directly test whether A_1Rs were required for PAP anti-nociception, we next i.t. injected hPAP into wild-type C57BL/6 and A_1-adenosine receptor knockout mice (*A*$_1$*R*$^{-/-}$, *Adora1*$^{-/-}$; backcrossed to C57BL/6 mice for 12 generations), then measured noxious thermal and mechanical sensitivity (Hua et al., 2007; Johansson et al., 2001). Strikingly, hPAP increased thermal paw withdrawal latency for three days in wild-type mice but was without effect in *A*$_1$*R*$^{-/-}$ mice (Figure 8A). Similarly, bPAP increased paw withdrawal latency to the noxious thermal stimulus in wild-type mice but had no effect in *A*$_1$*R*$^{-/-}$ mice (Figure S9). As expected, hPAP did not affect mechanical sensitivity in uninjured animals (Figure 8B).

We next tested wild-type and *A*$_1$*R*$^{-/-}$ mice using the CFA chronic inflammatory pain model and the SNI neuropathic pain model. Reproducing previous findings (Wu et al., 2005), *A*$_1$*R*$^{-/-}$ mice showed greater thermal hyperalgesia compared to wild-type mice after CFA injection and after nerve injury (but before PAP injection; Figure 8C, E). Following i.t. injection of hPAP, thermal and mechanical thresholds increased in the inflamed/injured paws of wild-type mice but not in *A*$_1$*R*$^{-/-}$ mice (Figure 8C–F). Likewise, the selective A_1R antagonist 8-cyclopentyl-1, 3-dipropylxanthine (CPX; 1 mg/kg, i.p.) transiently reversed the anti-nociceptive effects of hPAP in control and inflamed hindpaws (Figure S10). Conversely, injection (i.t.) of the selective A_1R agonist N^6-cyclopentyladenosine (CPA) into wild-type mice produced dose-dependent increases in paw withdrawal latency to our thermal stimulus (Figure S11), similar to i.t. hPAP. However unlike hPAP, CPA had short-term effects (lasting hours not days) and CPA caused transient paralysis at the two highest doses. When taken together, our results demonstrate that the anti-nociceptive effects of PAP are due to generation of adenosine followed by activation of A_1Rs. Moreover, our data demonstrate a novel *in vivo* function for PAP as an ectonucleotidase.

DISCUSSION

For seventy years, PAP was thought to be a secreted protein found only in the prostate and was used as a diagnostic marker for prostate cancer (Gutman and Gutman, 1938; Ostrowski and Kuciel, 1994). Despite years of research, little was known about how PAP functioned *in vivo* at a mechanistic level or which PAP substrate was most biologically relevant. In biochemical assays, PAP can dephosphorylate diverse substrates, including β-glycerophosphate, lysophosphatidic acid, phospho-amino acids and 5'-nucleotides (Dziembor-Gryszkiewicz et al., 1978; Li et al., 1984; Porvari et al., 1994; Tanaka et al., 2004; Vihko, 1978).

In our efforts to solve an old and unanswered question in the pain field, we found that PAP was expressed in nociceptive neurons, was anti-nociceptive and functioned as an ectonucleotidase. Importantly, we found that the *in vivo* effects of PAP were eliminated by deletion of one gene, the A_1-adenosine receptor. This makes it unlikely that PAP suppresses pain by generating any other molecules besides adenosine. Moreover, the *in vivo* effects of

PAP on acute and chronic pain mimic the effects of i.t. adenosine and A_1R agonists (Figure S11) (Liu and Salter, 2005; SSawynok, 2006). Notably, both PAP and adenosine receptor agonists have anti-allodynic and anti-hyperalgesic properties in animal models of inflammatory and neuropathic pain, both have a long (>24 h) duration of action after a single i.t. injection, and both lose their ability to suppress pain in $A_1R^{-/-}$ mice and following injection of A_1R antagonists (Belfrage et al., 1999; Cui et al., 1997; Eisenach et al., 2002; Gomes et al., 1999; Johansson et al., 2001; Lavand'homme and Eisenach, 1999; Lee and Yaksh, 1996; Maione et al., 2007; Poon and Sawynok, 1998). In addition, both $A_1R^{-/-}$ and $PAP^{-/-}$ mice show enhanced thermal hyperalgesia, but not enhanced allodynia, in neuropathic pain models (Figure 4C, D) (Wu et al., 2005). This shared modality-selective phenotype further supports our conclusion that endogenous PAP works via A_1R activation. Although our studies were focused on nociceptive neurons, PAP is expressed in many other tissues (Quintero et al., 2007) and thus could function as an ectonucleotidase throughout the body.

PAP has potent and long-lasting anti-nociceptive effects when compared to opioid analgesics

Morphine and other opioids are powerful analgesics but have side effects that limit their long-term use. We found that a single i.t. injection of hPAP (250 mU) produced an increase in paw withdrawal latency of 40.8 ± 3.3% (relative to baseline; n=74 mice) in the Hargreaves test (Figure S5C) and reproducibly lasted for three days (Figure 5, Figure 6, Figure 8, Figure S5A, S10). Using the same behavioral test, we found that 1 μg and 10 μg of morphine produced an increase in paw withdrawal latency of 24.9 ± 5.3% and 55.9 ± 13.7%, respectively, but lasted 1–4 h in mice (Figure S8). Similarly, others found that 1 μg and 10 μg of morphine (i.t., single dose) produced an increase in paw withdrawal latency of 36% and 60%, respectively (Dirig and Yaksh, 1995), that lasted hours in rats (Nishiyama et al., 2000; Zhang et al., 2005). Higher doses of i.t. morphine cause motor impairment and death (Figure S8) (Dirig and Yaksh, 1995; Grant et al., 1995; Nishiyama et al., 2000). Although high doses of A_1R agonists also cause motor impairment (Figure S11) (Sawynok, 2006), we found no such side-effects at the highest dose of PAP tested. These comparisons reveal that the magnitude of PAP and morphine anti-nociception is similar; however, PAP anti-nociception lasts substantially longer. In fact, using area under the curve (AUC) measurements that integrate magnitude of anti-nociception over time, the 250 mU dose of hPAP is eight-times more effective than the highest dose of morphine tested (Figures S5B, S8B). These long-lasting and A_1R-dependent anti-nociceptive effects of PAP are supported by previous studies showing that adenosine produces long-duration (>24 h) analgesia in humans and rodents (Belfrage et al., 1999; Eisenach et al., 2002; Lavand'homme and Eisenach, 1999). Lastly, we found that PAP anti-nociception could be *transiently* inhibited with an A_1R antagonist (Figure S10). This suggests that PAP is stable in spinal cord following injection and is capable of producing adenosine for days. Likewise, PAP has a very long (11.7 day) half-life in blood (Vihko et al., 1982).

PAP is the first molecularly-defined ectonucleotidase in nociceptive circuits

Nucleotides like ATP and ADP play key roles in pain mechanisms (Burnstock, 2007; Sawynok, 2006; Tozaki-Saitoh et al., 2008; Tsuda et al., 2005). Nucleotides are released extracellularly by stimulated sensory neurons and activate purinergic P2X and P2Y receptors on neurons and microglia. Activation of these receptors facilitates neurotransmission, sensitizes neurons and causes pain. The excitatory effects of extracellular nucleotides can be terminated by several membrane-bound and, in some cases, secreted ectonucleotidases. These ectonucleotidases dephosphorylate extracellular ATP, ADP and AMP to adenosine (Zimmermann, 2006). While ATP has excitatory effects and causes pain, adenosine has inhibitory effects and suppresses pain (Nakagawa et al., 2007; Sawynok, 2006).

One or more ectonucleotidases were known to exist in nociceptive circuits (Nagy and Daddona, 1985; Scott, 1967; Suran, 1974). Considering the key roles nucleotides and adenosine play in pain mechanisms, it is surprising to note that none of these ectonucleotidases have been molecularly identified. Using electrophysiological approaches, two groups found that application of ATP, ADP or AMP inhibited postsynaptic neurons in the dorsal spinal cord indirectly via metabolic conversion to adenosine (Li and Perl, 1995; Salter and Henry, 1985). Likewise, Patterson and colleagues used indwelling microprobes and found that adenosine was metabolically generated *in vivo* when the dorsal spinal cord was perfused with AMP (Patterson et al., 2001). Dephosphorylation of AMP to adenosine was partially blocked by co-perfusion with α,β-methylene-ADP (Patterson et al., 2001), an inhibitor of ecto-5'-nucleotidase (CD73). This enzyme has not yet been molecularly-characterized in DRG neurons or spinal cord.

Our studies clearly show that PAP is expressed in small-diameter DRG neurons, that PAP dephosphorylates AMP to adenosine *in vitro*, in heterologous cells, in DRG neurons and in lamina II of the spinal cord, and that PAP anti-nociception requires A_1Rs. To our knowledge, none of the known ectonucleotidases (Zimmermann, 2006) have been studied at this level of detail in nociceptive circuits. Collectively, this makes PAP the first molecularly-defined ectonucleotidase in nociceptive circuits.

PAP is well-localized to modulate A_1-adenosine receptors in spinal cord lamina II

Our data highlight a close functional relationship between PAP and A_1Rs. This raises the question of where PAP acts to modulate A_1Rs and nociceptive behaviors. Within the spinal cord, A_1Rs are concentrated in lamina II, particularly on postsynaptic neurons that are in close contact with $IB4^+$ axon terminals, but not in close contact with $CGRP^+$ axon terminals (Schulte et al., 2003). A_1Rs are also found presynaptically in small- to medium-diameter DRG neurons, and possibly in the axon terminals of these neurons (based on accumulation of A_1Rs proximal to dorsal root ligature) (Schulte et al., 2003). In addition, A_1R activation inhibits presynaptic glutamate release primarily from unmyelinated terminals and inhibits postsynaptic neurons in the substantia gelatinosa (lamina II) of spinal cord (Lao et al., 2001; Li and Perl, 1994; Patel et al., 2001).

Considering that virtually all PAP^+ neurons and axons are $IB4^+$ (Table S1) and terminate in lamina II (Figure S4), this makes PAP well-localized to generate extracellular adenosine and modulate A_1Rs on presynaptic terminals and on postsynaptic neurons in the IB4-binding region of lamina II. In addition, PAP (TMPase) is enriched on the presynaptic membranes of DRG neurons at the level of electron microscopy (Knyihar-Csillik et al., 1986) and has a broad pH optimum (pH 3–8) (Van Etten, 1982), making PAP capable of generating adenosine locally at synapses.

Further support for a central site of action comes from the fact that dephosphoryation of extracellular AMP in lamina II is reduced in $PAP^{-/-}$ mice and PAP is anti-nociceptive when injected intraspinally. Moreover, central injection of PAP can rescue behavioral deficits caused by deletion of PAP throughout the animal (Figure 6).

Although our data clearly support a central mechanism of action, we cannot exclude the possibility that PAP might also generate adenosine peripherally to mediate anti-nociception. Peripheral administration of adenosine has long-lasting anti-nociceptive and analgesic effects in rodents and humans, just like central administration (Hayashida et al., 2005; Sawynok, 2006). We detected PAP on axons in the dermis of the skin; however, our antibody was not sensitive enough to detect PAP on axon terminals in epidermis (B.T-B. and M.J.Z, unpublished). Moreover, others found that TMPase (PAP) accumulated proximal to a ligature of the sural nerve, suggesting PAP is transported peripherally (McMahon and Moore, 1988).

Physiological function of PAP throughout the body – insights from pain-sensing neurons

In prostate, PAP is thought to function as a tumor suppressor. Notably, prostate cancer cell growth rate is reduced when secretory hPAP (referred to as "cellular" PAP by the authors) is overexpressed (Lin et al., 1992; Meng and Lin, 1998; Veeramani et al., 2005). Conversely, deletion of PAP (secreted and TM isoforms) in mice leads to prostate hyperplasia followed by prostate cancer (Vihko et al., abstract from Proceedings of the AACR, 2005). The mechanism by which PAP mediates growth suppression is, at present, unclear. Correlative data from Lin and colleagues suggests secretory ("cellular") PAP regulates growth directly by dephosphorylating phosphotyrosine residues in the cytoplasmic tail of ErbB2 (Veeramani et al., 2005). This direct mechanism seems unlikely, particularly since the cytoplasmic tail of ErbB2 is not accessible to the active site of secretory PAP (which is located extracellularly (Figure 1A) and in the lumen of vesicles). Instead, PAP could *indirectly* regulate proliferation by generating adenosine.

In support of this, there are four adenosine receptor subtypes, with A_1 and A_3 coupled to inhibitory G_i-proteins and A_{2a} and A_{2b} coupled to stimulatory G_q- and G_s-proteins (Jacobson and Gao, 2006). PAP could differentially modulate intracellular signaling depending upon which adenosine receptor subtypes are expressed by cells. Notably, A_3-adenosine receptors are found on prostate cancer cells and A_3-agonists inhibit the growth of these cells (Fishman et al., 2003).

Adenosine regulates many other physiological processes besides pain and cancer, including anxiety, inflammation, blood pressure, pulmonary function and renal function (Jacobson and Gao, 2006). TM-PAP is expressed throughout the body (Quintero et al., 2007). As such, TM-PAP could regulate diverse physiological processes that are dependent on adenosine. Lastly, our study overturns the long-held belief that PAP is a generic "acid phosphatase" by discovering a specific *in vivo* function for PAP as an ectonucleotidase.

EXPERIMENTAL PROCEDURES

All procedures and behavioral experiments involving vertebrate animals were approved by Institutional Animal Care and Use Committees at the University of North Carolina at Chapel Hill and at the Universities of Oulu and Helsinki.

Molecular Biology

The full-length expression construct of PAP-transmembrane isoform (nt 64–1317 from GenBank accession # NM_207668) was generated by RT-PCR amplification, using C57BL/6 mouse trigeminal cDNA as template and Phusion polymerase. PCR products were cloned into pcDNA3.1 and completely sequenced. Isoform-specific *in situ* hybridization probes of PAP, secreted variant (nt 1544–2625 from GenBank accession # NM_019807) and PAP, transmembrane variant (nt 1497–2577 from GenBank accession # NM_207668) were generated by PCR amplification, using C57BL/6 mouse genomic DNA as template and Phusion polymerase, then cloned into pBluescript-KS.

In situ hybridization was performed as described previously using digoxygenin-labeled antisense and sense (control) riboprobes (Dong et al., 2001).

We confirmed that PAP was expressed in human DRG by performing RT-PCR with RNA from human DRG (Clontech) and primers that spanned three introns (exon 6 primer: 5' ctttcaggattacatggccagg and exon 9 primer: 5' cgtcaagtggcaagaagcatag).

Tissue Preparation

Adult male mice, 6–12 weeks of age, were sacrificed by cervical dislocation, decapitation or pentobarbital overdose. Lumbar spinal cord and DRG (L4–L6) were dissected, and then postfixed for 8 h and 2 h, respectively. Tissues were cryoprotected in 20% sucrose, 0.1 M phosphate buffer, pH 7.3 at 4°C for 24 hours, frozen in OCT, sectioned with a cryostat at 15–20 μm, and mounted on Superfrost Plus slides. Slides were stored at −20°C. Free-floating sections were sectioned at 30 μm and immediately stained.

Histology

Enzyme histochemistry was performed essentially as described by Shields et al., with modifications suggested by Silverman and Kruger (Shields et al., 2003; Silverman and Kruger, 1988a). Briefly, cells or tissue sections were washed twice with 40 mM Trizma-Maleate (TM) buffer, pH 5.6., then once with TM buffer containing 8% (w/v) sucrose. Samples were then incubated at 37°C for 2 h in TM buffer containing 8% sucrose (w/v), 6 mM thiamine monophosphate chloride or adenosine monophosphate (0.3 mM for tissue sections, 6 mM for HEK 293 cells), and 2.4 mM lead nitrate. Lead nitrate must be made fresh immediately prior to use. To reduce non-specific background staining, samples were washed once with 2% acetic acid for one minute. Samples were then washed three times with TM buffer, developed for 10 seconds with 1% sodium sulfide, washed several times with PBS, pH 7.4, and mounted in Gel/Mount (Biomeda). When assaying HEK 293 cells using TMP or AMP histochemistry, we stained duplicate samples with and without 0.1% Triton X-100 in the initial TM wash. Images were acquired using a Zeiss Axioskop and Olympus DP-71 camera.

Immunofluorescence was performed using antibodies and procedures as previously described (Zylka et al., 2005). Additional antibodies included: 1:250 mouse anti-NeuN (MAB377, Chemicon), 1:300 guinea pig anti-P2X3 (GP10108, Neuromics), 1:1000 goat anti-VR1 (sc-12498, Santa Cruz) and 1:1000 rabbit anti-human PAP (Biomeda). We found it was necessary to amplify the anti-PAP antibody signal by using secondary antibodies conjugated to biotin, then using either 1:250 Streptavidin-Cy3 (Jackson) or the Tyramide Signal Amplification kit (New England Nuclear, following manufacturers protocol). Images were obtained using a Leica TCS-NT confocal microscope.

Injections and Drugs

For intrathecal drug delivery, 5 μL was injected into unanesthetized mice using the direct lumbar puncture method (Fairbanks, 2003). Human PAP (Sigma, P1774, 100 U/mL) was dialyzed against 0.9% saline using Slide-A-Lyzer Mini dialysis units (Pierce, 69576) for 4 hours at 4°C. After dialysis, samples were diluted in 0.9% saline to a final concentration of 1.3 mg/mL (50 U/mL) and stored at −80°C. hPAP was heat-inactivated by incubating at 65°C for 40 min. Bovine prostatic acid phosphatase (bPAP, Sigma, P6409) was dissolved (aided by sonication) in 0.9% saline to a final concentration of 30 mg/mL (0.3 U/mL). Enzyme activity was quantified using the EnzChek Phosphatase Assay Kit (Invitrogen, E12020) following the manufacturer's protocol. Bovine serum albumin (BSA, Sigma, A3912) was dissolved in 0.9% saline to a final concentration of 1.3 mg/mL. Recombinant bovine alkaline phosphatase was purchased from Sigma (P8361, expressed in *Pichia pastoris*, >4000 U/mg protein). Morphine sulfate (Sigma, M8777) and N^6-cyclopentyladenosine (Sigma, C8031; 10 mM stock in dimethylsulfoxide (DMSO)) were diluted into 0.9% saline. 8-cyclopentyl-1, 3-dipropylxanthine (C101, Sigma) was dissolved in 0.9% saline containing 5% DMSO, 1.25% 1 M NaOH and injected i.p.

Behavior

$PAP^{-/-}$ and $A_1R^{-/-}$ mice were backcrossed to C57BL/6 mice (Jackson) for 10 and 12 generations, respectively. Isogenic wild-type mice were then derived from the $PAP^{-/-}$ line and used as wild-type controls. C57BL/6 male mice were purchased from Jackson Laboratories for all behavioral experiments involving PAP protein injections. Unless indicated otherwise, male mice, 2–4 months old, were used for all behavioral experiments. All mice were acclimated to the testing room, equipment and experimenter for one to three days before behavioral testing. The experimenter was blind to genotype and drug treatment during behavioral testing.

Thermal sensitivity was measured by heating one hindpaw with a Plantar Test apparatus (IITC) following the Hargreaves method (Hargreaves et al., 1988). The radiant heat source intensity was calibrated so that a paw withdrawal reflex was evoked in ~10 s., on average, in wild-type C57BL/6 mice. Cutoff time was 20 s. One measurement was taken from each paw per day to determine paw withdrawal latency (with the exception of our morphine and CPA dose-response experiments which required multiple measurements per day). To perform the tail immersion assay, mice were gently restrained in a towel and the distal one-third of the tail was immersed in 46.5°C or 49°C water. Latency to withdrawal the tail was measured once per mouse. For the hot plate test, mice were placed on a metal surface heated at 52°C and latency to jump, lick paws or shake paws was measured. Mechanical sensitivity was measured using semi-flexible tips attached to an Electronic von Frey apparatus (IITC) as described elsewhere (Cunha et al., 2004; Inoue et al., 2004). Three measurements were taken from each paw (separated at 10 min intervals) then averaged to determine paw withdrawal threshold in grams.

To induce inflammatory pain, 20 μL Complete Freunds Adjuvant (CFA, from Sigma or MP Biomedicals) was injected into one hindpaw, centrally beneath glabrous skin, with a 30G needle. The spared nerve injury (SNI) model of neuropathic pain was performed as described (Shields et al., 2003).

Supplementary Material

Refer to Web version on PubMed Central for supplementary material.

REFERENCES

Belfrage M, Segerdahl M, Arner S, Sollevi A. The safety and efficacy of intrathecal adenosine in patients with chronic neuropathic pain. Anesth Analg 1999;89:136–142. [PubMed: 10389791]

Burnstock G. Physiology and pathophysiology of purinergic neurotransmission. Physiol Rev 2007;87:659–797. [PubMed: 17429044]

Carr PA, Yamamoto T, Nagy JI. Calcitonin gene-related peptide in primary afferent neurons of rat: co-existence with fluoride-resistant acid phosphatase and depletion by neonatal capsaicin. Neuroscience 1990;36:751–760. [PubMed: 2234408]

Colmant HJ. Aktivitatsschwankungen der sauren phosphatase im ruckenmark und den spinalganglien der ratte nach durchschneidung des nervus ischiadicus. Arch Psychiat Nervnekr 1959;199:60–71.

Costigan M, Befort K, Karchewski L, Griffin RS, D'Urso D, Allchorne A, Sitarski J, Mannion JW, Pratt RE, Woolf CJ. Replicate high-density rat genome oligonucleotide microarrays reveal hundreds of regulated genes in the dorsal root ganglion after peripheral nerve injury. BMC Neurosci 2002;3:16. [PubMed: 12401135]

Csillik, B.; Knyihar-Csillik, E. The Protean Gate: Structure and plasticity of the primary nociceptive analyzer. Budapest: Akademiai Kiado; 1986.

Cui JG, Sollevi A, Linderoth B, Meyerson BA. Adenosine receptor activation suppresses tactile hypersensitivity and potentiates spinal cord stimulation in mononeuropathic rats. Neurosci Lett 1997;223:173–176. [PubMed: 9080460]

Cunha TM, Verri WA Jr, Vivancos GG, Moreira IF, Reis S, Parada CA, Cunha FQ, Ferreira SH. An electronic pressure-meter nociception paw test for mice. Braz J Med Biol Res 2004;37:401–407. [PubMed: 15060710]

Dalsgaard CJ, Ygge J, Vincent SR, Ohrling M, Dockray GJ, Elde R. Peripheral projections and neuropeptide coexistence in a subpopulation of fluoride-resistant acid phosphatase reactive spinal primary sensory neurons. Neurosci Lett 1984;51:139–144. [PubMed: 6096769]

Davis-Taber RA. Transcriptional profiling of dorsal root ganglia in a neuropathic pain model using microarray and laser capture microdissection. Drug Dev Res 2006;67:308–330.

Dirig DM, Yaksh TL. Differential right shifts in the dose-response curve for intrathecal morphine and sufentanil as a function of stimulus intensity. Pain 1995;62:321–328. [PubMed: 8657432]

Dodd J, Jahr CE, Hamilton PN, Heath MJ, Matthew WD, Jessell TM. Cytochemical and physiological properties of sensory and dorsal horn neurons that transmit cutaneous sensation. Cold Spring Harb Symp Quant Biol 1983;48(Pt 2):685–695. [PubMed: 6327172]

Dong X, Han S, Zylka MJ, Simon MI, Anderson DJ. A diverse family of GPCRs expressed in specific subsets of nociceptive sensory neurons. Cell 2001;106:619–632. [PubMed: 11551509]

Dziembor-Gryszkiewicz E, Fikus M, Kazimierczuk Z, Ostrowski W. Activity of human prostatic acid phosphatase toward purine 5'-phosphonucleosides. Bull Acad Pol Sci Biol 1978;26:815–821. [PubMed: 752405]

Eisenach JC, Hood DD, Curry R. Preliminary efficacy assessment of intrathecal injection of an American formulation of adenosine in humans. Anesthesiology 2002;96:29–34. [PubMed: 11752998]

Fairbanks CA. Spinal delivery of analgesics in experimental models of pain and analgesia. Adv Drug Deliv Rev 2003;55:1007–1041. [PubMed: 12935942]

Fishman P, Bar-Yehuda S, Ardon E, Rath-Wolfson L, Barrer F, Ochaion A, Madi L. Targeting the A3 adenosine receptor for cancer therapy: inhibition of prostate carcinoma cell growth by A3AR agonist. Anticancer Res 2003;23:2077–2083. [PubMed: 12894581]

Gomes JA, Li X, Pan HL, Eisenach JC. Intrathecal adenosine interacts with a spinal noradrenergic system to produce antinociception in nerve-injured rats. Anesthesiology 1999;91:1072–1079. [PubMed: 10519511]

Grant GJ, Cascio M, Zakowski MI, Langerman L, Turndorf H. Intrathecal administration of liposomal morphine in a mouse model. Anesth Analg 1995;81:514–518. [PubMed: 7653814]

Gutman AB, Gutman EB. An "acid" phosphatase occurring in the serum of patients with metastasizing carcinoma of the prostate gland. J Clin Invest 1938;17:473–478. [PubMed: 16694594]

Hargreaves K, Dubner R, Brown F, Flores C, Joris J. A new and sensitive method for measuring thermal nociception in cutaneous hyperalgesia. Pain 1988;32:77–88. [PubMed: 3340425]

Hayashida M, Fukuda K, Fukunaga A. Clinical application of adenosine and ATP for pain control. J Anesth 2005;19:225–235. [PubMed: 16032451]

Hua X, Erikson CJ, Chason KD, Rosebrock CN, Deshpande DA, Penn RB, Tilley SL. Involvement of A1 adenosine receptors and neural pathways in adenosine-induced bronchoconstriction in mice. Am J Physiol Lung Cell Mol Physiol 2007;293:L25–L32. [PubMed: 17468137]

Hunt SP, Mantyh PW. The molecular dynamics of pain control. Nat Rev Neurosci 2001;2:83–91. [PubMed: 11252998]

Hunt SP, Rossi J. Peptide- and non-peptide-containing unmyelinated primary afferents: the parallel processing of nociceptive information. Philos Trans R Soc Lond B Biol Sci 1985;308:283–289. [PubMed: 2580323]

Inoue M, Rashid MH, Fujita R, Contos JJ, Chun J, Ueda H. Initiation of neuropathic pain requires lysophosphatidic acid receptor signaling. Nat Med 2004;10:712–718. [PubMed: 15195086]

Jacobson KA, Gao ZG. Adenosine receptors as therapeutic targets. Nat Rev Drug Discov 2006;5:247–264. [PubMed: 16518376]

Johansson B, Halldner L, Dunwiddie TV, Masino SA, Poelchen W, Gimenez-Llort L, Escorihuela RM, Fernandez-Teruel A, Wiesenfeld-Hallin Z, Xu XJ, et al. Hyperalgesia, anxiety, and decreased hypoxic neuroprotection in mice lacking the adenosine A1 receptor. Proc Natl Acad Sci U S A 2001;98:9407–9412. [PubMed: 11470917]

Knyihar-Csillik E, Bezzegh A, Boti S, Csillik B. Thiamine monophosphatase: a genuine marker for transganglionic regulation of primary sensory neurons. J Histochem Cytochem 1986;34:363–371. [PubMed: 3005391]

Lao LJ, Kumamoto E, Luo C, Furue H, Yoshimura M. Adenosine inhibits excitatory transmission to substantia gelatinosa neurons of the adult rat spinal cord through the activation of presynaptic A(1) adenosine receptor. Pain 2001;94:315–324. [PubMed: 11731068]

Lavand'homme PM, Eisenach JC. Exogenous and endogenous adenosine enhance the spinal antiallodynic effects of morphine in a rat model of neuropathic pain. Pain 1999;80:31–36. [PubMed: 10204715]

Lazarowski ER, Tarran R, Grubb BR, van Heusden CA, Okada S, Boucher RC. Nucleotide release provides a mechanism for airway surface liquid homeostasis. J Biol Chem 2004;279:36855–36864. [PubMed: 15210701]

Lee YW, Yaksh TL. Pharmacology of the spinal adenosine receptor which mediates the antiallodynic action of intrathecal adenosine agonists. J Pharmacol Exp Ther 1996;277:1642–1648. [PubMed: 8667233]

Li HC, Chernoff J, Chen LB, Kirschonbaum A. A phosphotyrosyl-protein phosphatase activity associated with acid phosphatase from human prostate gland. Eur J Biochem 1984;138:45–51. [PubMed: 6319132]

Li J, Perl ER. Adenosine inhibition of synaptic transmission in the substantia gelatinosa. J Neurophysiol 1994;72:1611–1621. [PubMed: 7823090]

Li J, Perl ER. ATP modulation of synaptic transmission in the spinal substantia gelatinosa. J Neurosci 1995;15:3357–3365. [PubMed: 7751915]

Lin MF, DaVolio J, Garcia-Arenas R. Expression of human prostatic acid phosphatase activity and the growth of prostate carcinoma cells. Cancer Res 1992;52:4600–4607. [PubMed: 1380886]

Liu XJ, Salter MW. Purines and pain mechanisms: recent developments. Curr Opin Investig Drugs 2005;6:65–75.

Maione S, de Novellis V, Cappellacci L, Palazzo E, Vita D, Luongo L, Stella L, Franchetti P, Marabese I, Rossi F, Grifantini M. The antinociceptive effect of 2-chloro-2'-C-methyl-N6-cyclopentyladenosine (2'-Me-CCPA), a highly selective adenosine A1 receptor agonist, in the rat. Pain 2007;131:281–292. [PubMed: 17317007]

McMahon SB, Moore CE. Plasticity of primary afferent acid phosphatase expression following rerouting of afferents from muscle to skin in the adult rat. J Comp Neurol 1988;274:1–8. [PubMed: 3417905]

Meng TC, Lin MF. Tyrosine phosphorylation of c-ErbB-2 is regulated by the cellular form of prostatic acid phosphatase in human prostate cancer cells. J Biol Chem 1998;273:22096–22104. [PubMed: 9705354]

Nagy JI, Daddona PE. Anatomical and cytochemical relationships of adenosine deaminase-containing primary afferent neurons in the rat. Neuroscience 1985;15:799–813. [PubMed: 2415872]

Nagy JI, Hunt SP. Fluoride-resistant acid phosphatase-containing neurones in dorsal root ganglia are separate from those containing substance P or somatostatin. Neuroscience 1982;7:89–97. [PubMed: 6176904]

Nakagawa T, Wakamatsu K, Zhang N, Maeda S, Minami M, Satoh M, Kaneko S. Intrathecal administration of ATP produces long-lasting allodynia in rats: differential mechanisms in the phase of the induction and maintenance. Neuroscience 2007;147:445–455. [PubMed: 17543465]

Nishiyama T, Ho RJ, Shen DD, Yaksh TL. The effects of intrathecal morphine encapsulated in L- and D-dipalmitoylphosphatidyl choline liposomes on acute nociception in rats. Anesth Analg 2000;91:423–428. [PubMed: 10910861]

Ostrowski WS, Kuciel R. Human prostatic acid phosphatase: selected properties and practical applications. Clin Chim Acta 1994;226:121–129. [PubMed: 7923807]

Patel MK, Pinnock RD, Lee K. Adenosine exerts multiple effects in dorsal horn neurones of the adult rat spinal cord. Brain Res 2001;920:19–26. [PubMed: 11716807]

Patterson SL, Sluka KA, Arnold MA. A novel transverse push-pull microprobe: in vitro characterization and in vivo demonstration of the enzymatic production of adenosine in the spinal cord dorsal horn. J Neurochem 2001;76:234–246. [PubMed: 11145997]

Poon A, Sawynok J. Antinociception by adenosine analogs and inhibitors of adenosine metabolism in an inflammatory thermal hyperalgesia model in the rat. Pain 1998;74:235–245. [PubMed: 9520238]

Porvari KS, Herrala AM, Kurkela RM, Taavitsainen PA, Lindqvist Y, Schneider G, Vihko PT. Site-directed mutagenesis of prostatic acid phosphatase. Catalytically important aspartic acid 258, substrate specificity, and oligomerization. J Biol Chem 1994;269:22642–22646. [PubMed: 8077215]

Post C. Antinociceptive effects in mice after intrathecal injection of 5'-N-ethylcarboxamide adenosine. Neurosci Lett 1984;51:325–330. [PubMed: 6097841]

Quintero IB, Araujo CL, Pulkka AE, Wirkkala RS, Herrala AM, Eskelinen EL, Jokitalo E, Hellstrom PA, Tuominen HJ, Hirvikoski PP, Vihko PT. Prostatic acid phosphatase is not a prostate specific target. Cancer Res 2007;67:6549–6554. [PubMed: 17638863]

Roiko K, Janne OA, Vihko P. Primary structure of rat secretory acid phosphatase and comparison to other acid phosphatases. Gene 1990;89:223–229. [PubMed: 2373368]

Salter MW, Henry JL. Effects of adenosine 5'-monophosphate and adenosine 5'-triphosphate on functionally identified units in the cat spinal dorsal horn. Evidence for a differential effect of adenosine 5'-triphosphate on nociceptive vs non-nociceptive units. Neuroscience 1985;15:815–825. [PubMed: 2999643]

Sanyal S, Rustioni A. Phosphatases in the substantia gelatinosa and motoneurones: a comparative histochemical study. Brain Res 1974;76:161–166. [PubMed: 4367402]

Sawynok J. Adenosine and ATP receptors. Handb Exp Pharmacol 2006:309–328.

Schulte G, Robertson B, Fredholm BB, DeLander GE, Shortland P, Molander C. Distribution of antinociceptive adenosine A1 receptors in the spinal cord dorsal horn, and relationship to primary afferents and neuronal subpopulations. Neuroscience 2003;121:907–916. [PubMed: 14580941]

Scott TG. The distribution of 5'-nucleotidase in the brain of the mouse. J Comp Neurol 1967;129:97–114.

Shields SD, Eckert WA 3rd, Basbaum AI. Spared nerve injury model of neuropathic pain in the mouse: a behavioral and anatomic analysis. J Pain 2003;4:465–470. [PubMed: 14622667]

Silverman JD, Kruger L. Acid phosphatase as a selective marker for a class of small sensory ganglion cells in several mammals: spinal cord distribution, histochemical properties, and relation to fluoride-resistant acid phosphatase (FRAP) of rodents. Somatosens Res 1988a;5:219–246. [PubMed: 3128853]

Silverman JD, Kruger L. Lectin and neuropeptide labeling of separate populations of dorsal root ganglion neurons and associated "nociceptor" thin axons in rat testis and cornea whole-mount preparations. Somatosens Res 1988b;5:259–267. [PubMed: 3358044]

Silverman JD, Kruger L. Selective neuronal glycoconjugate expression in sensory and autonomic ganglia: relation of lectin reactivity to peptide and enzyme markers. J Neurocytol 1990;19:789–801. [PubMed: 2077115]

Suran AA. 5'-Nucleotidase and an acid phosphatase of spinal cord. Comparative histochemistry and specificity of the enzymes in mouse and cat spinal cords. Cytologic localization in mouse substantia gelatinosa. J Histochem Cytochem 1974;22:802–811. [PubMed: 4212518]

Tanaka M, Kishi Y, Takanezawa Y, Kakehi Y, Aoki J, Arai H. Prostatic acid phosphatase degrades lysophosphatidic acid in seminal plasma. FEBS Lett 2004;571:197–204. [PubMed: 15280042]

Tenser RB. Sequential changes of sensory neuron (fluoride-resistant) acid phosphatase in dorsal root ganglion neurons following neurectomy and rhizotomy. Brain Res 1985;332:386–389. [PubMed: 3995277]

Tenser RB, Viselli AL, Savage DH. Reversible decrease of fluoride resistant acid phosphatase-positive neurons after herpes simplex virus infection. Neurosci Lett 1991;130:85–88. [PubMed: 1749519]

Tozaki-Saitoh H, Tsuda M, Miyata H, Ueda K, Kohsaka S, Inoue K. P2Y12 receptors in spinal microglia are required for neuropathic pain after peripheral nerve injury. J Neurosci 2008;28:4949–4956. [PubMed: 18463248]

Tsuda M, Inoue K, Salter MW. Neuropathic pain and spinal microglia: a big problem from molecules in "small" glia. Trends Neurosci 2005;28:101–107. [PubMed: 15667933]

Van Etten RL. Human prostatic acid phosphatase: a histidine phosphatase. Ann N Y Acad Sci 1982;390:27–51. [PubMed: 6124201]

Veeramani S, Yuan TC, Chen SJ, Lin FF, Petersen JE, Shaheduzzaman S, Srivastava S, MacDonald RG, Lin MF. Cellular prostatic acid phosphatase: a protein tyrosine phosphatase involved in androgen-

independent proliferation of prostate cancer. Endocr Relat Cancer 2005;12:805–822. [PubMed: 16322323]

Vihko P. Characterization of the principal human prostatic acid phosphatase isoenzyme, purified by affinity chromatography and isoelectric focusing. Part II. Clin Chem 1978;24:1783–1787.

Vihko P. Human prostatic acid phosphatases: purification of a minor enzyme and comparisons of the enzymes. Invest Urol 1979;16:349–352. [PubMed: 429130]

Vihko P, Schroeder FH, Lukkarinen O, Vihko R. Secretion into and elimination from blood circulation of prostate specific acid phosphatase, measured by radioimmunoassay. J Urol 1982;128:202–204. [PubMed: 6180187]

Woolf CJ, Ma Q. Nociceptors--noxious stimulus detectors. Neuron 2007;55:353–364. [PubMed: 17678850]

Wu WP, Hao JX, Halldner L, Lovdahl C, DeLander GE, Wiesenfeld-Hallin Z, Fredholm BB, Xu XJ. Increased nociceptive response in mice lacking the adenosine A1 receptor. Pain 2005;113:395–404. [PubMed: 15661449]

Zhang Y, Conklin DR, Li X, Eisenach JC. Intrathecal morphine reduces allodynia after peripheral nerve injury in rats via activation of a spinal A1 adenosine receptor. Anesthesiology 2005;102:416–420. [PubMed: 15681960]

Zimmermann H. Ectonucleotidases in the nervous system. Novartis Found Symp 2006;276:113–128. [PubMed: 16805426]discussion 128-130, 233-117, 275-181

Zylka MJ, Rice FL, Anderson DJ. Topographically distinct epidermal nociceptive circuits revealed by axonal tracers targeted to Mrgprd. Neuron 2005;45:17–25. [PubMed: 15629699]

ACKNOWLEDGMENTS

We thank Edward Perl, Paul Farel and Ben Philpot for comments on the manuscript, David J. Anderson for providing *Mrgprd*Δ^{EGFPf} mice, Stephen L. Tilley for providing isogenic $A_1R^{-/-}$ mice, Eduardo R. Lazarowski for measuring adenosine and adenine nucleotides by HPLC, Shannon Shields and Allan I. Basbaum for teaching us how to perform pain behavioral assays and SNI surgeries and Yvette Chuang and Kunjumon Vadakkan for excellent technical assistance. This work was supported by UNC startup funds, grants to M.J.Z. from The Sloan Foundation, The Searle Scholars Program, The Klingenstein Foundation, The Whitehall Foundation, Rita Allen Foundation and NINDS (R01NS060725), a grant to N.A.S. from NINDS (F30NS063507) and grants to P.V. from The Sigrid Juselius Foundation, The Finnish Cancer Foundation and The Research Council for Medicine of the Academy of Finland. Confocal imaging was performed at the UNC-CH Confocal Imaging Facility, which is co-funded by NINDS and NICHD (P30NS045892). M.J.Z. is a Rita Allen Foundation Milton E. Cassel Scholar.

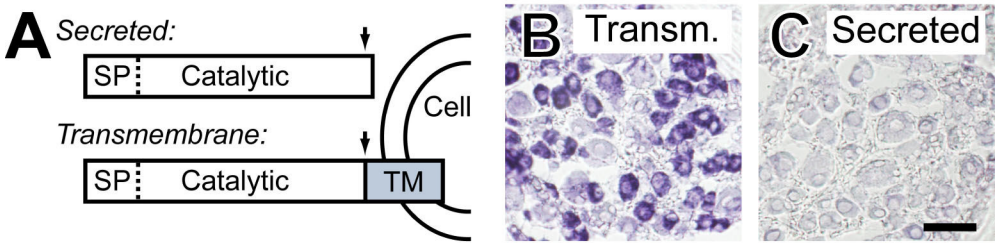

Figure 1. DRG neurons express the transmembrane isoform of PAP

(A) Secreted and transmembrane isoforms of PAP. Both isoforms have identical N-terminal regions, including the signal peptide (SP) and extracellular catalytic acid phosphatase domain. Alternative splicing at the last intron-exon junction (arrow) results in the inclusion or exclusion of a transmembrane (TM) domain. (B, C) *In situ* hybridization of mouse lumbar DRG with riboprobes complimentary to the unique 3' untranslated regions of (B) the transmembrane isoform or (C) the secreted isoform. Scale bar: 50 μm in B, C.

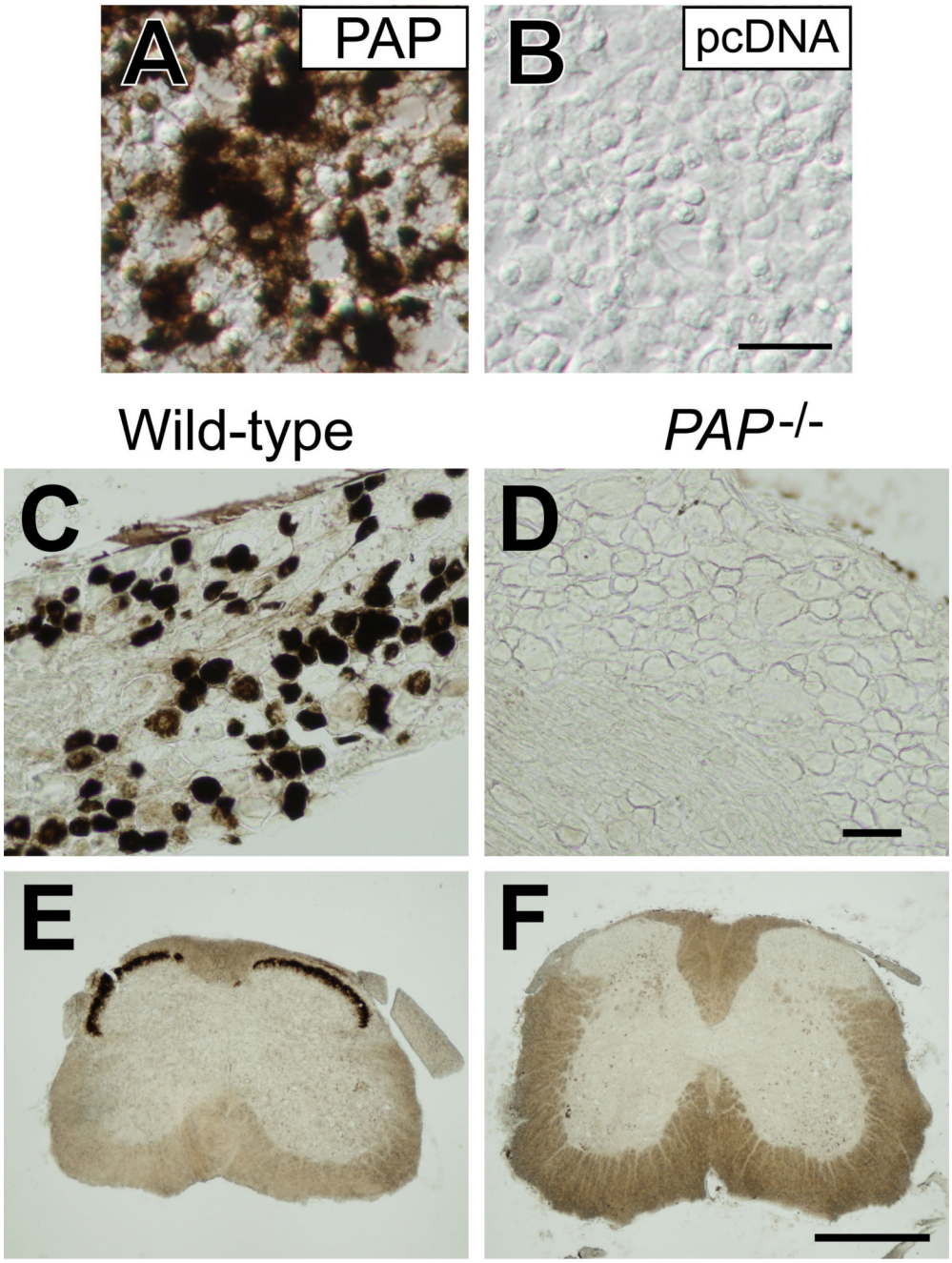

Figure 2. PAP dephosphorylates TMP in HEK 293 cells and nociceptive circuits

(A) HEK 293 cells were transfected with a mouse TM-PAP expression construct or (B) with empty pcDNA3.1 vector and then stained using TMP histochemistry. The plasma membrane was not permeabilized so that extracellular phosphatase activity could be assayed. (C–D) Lumbar DRG and (E–F) spinal cord from wild-type and *PAP*$^{-/-}$ adult mice stained using TMP histochemistry. Identical results were obtained from fourteen additional mice of each genotype. TMP (6 mM) was used as substrate and buffer pH was 5.6 in all panels. Scale bar: 50 μm in A–D; 500 μm in E, F.

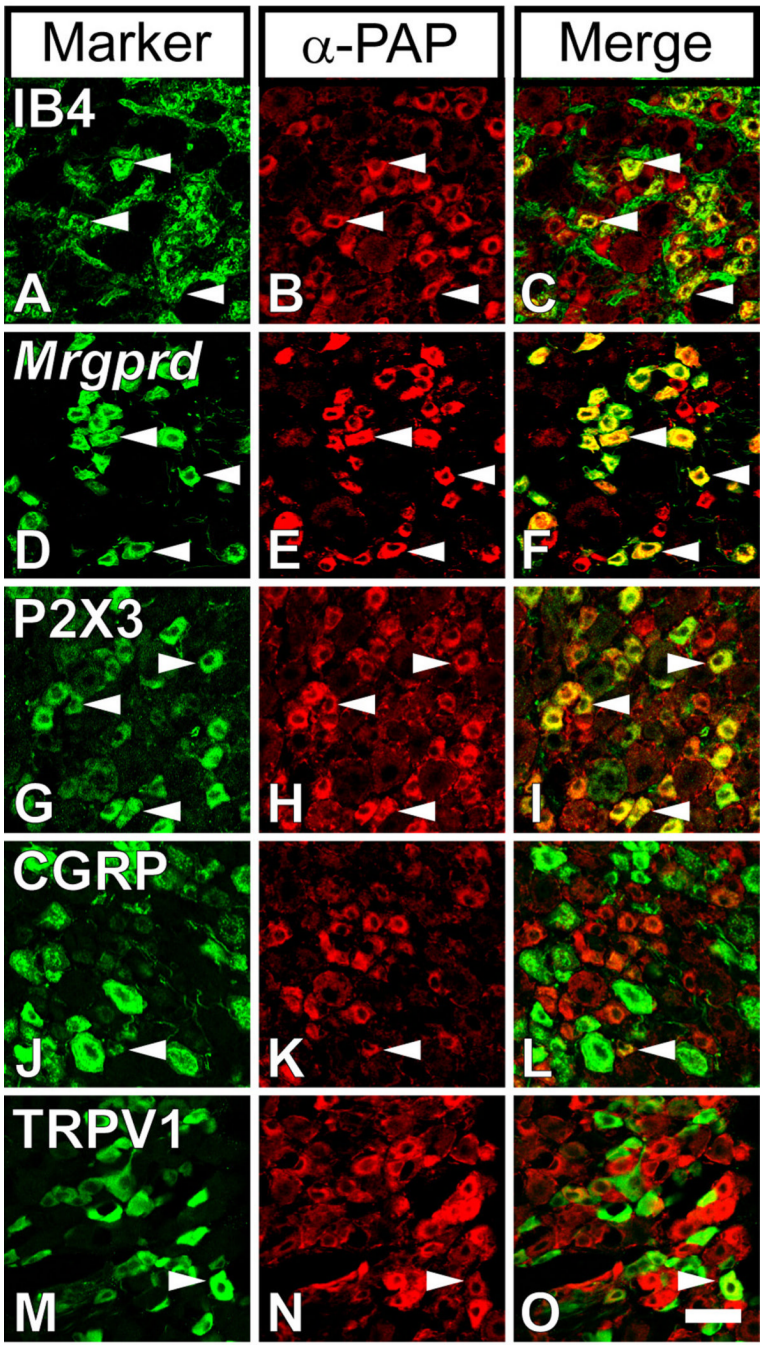

Figure 3. PAP is primarily expressed in nonpeptidergic neurons

(A–O) Mouse L4–L6 DRG neurons were stained with antibodies against various sensory neuron markers (green) and with antibodies against PAP (red). Tissue from adult *Mrgprd*Δ^{EGFPf} mice was used to identify *Mrgprd*-expressing neurons. Arrowheads mark examples of double-labeled cells. Images were acquired by confocal microscopy. Scale bar (bottom right panel): 50 μm for all panels.

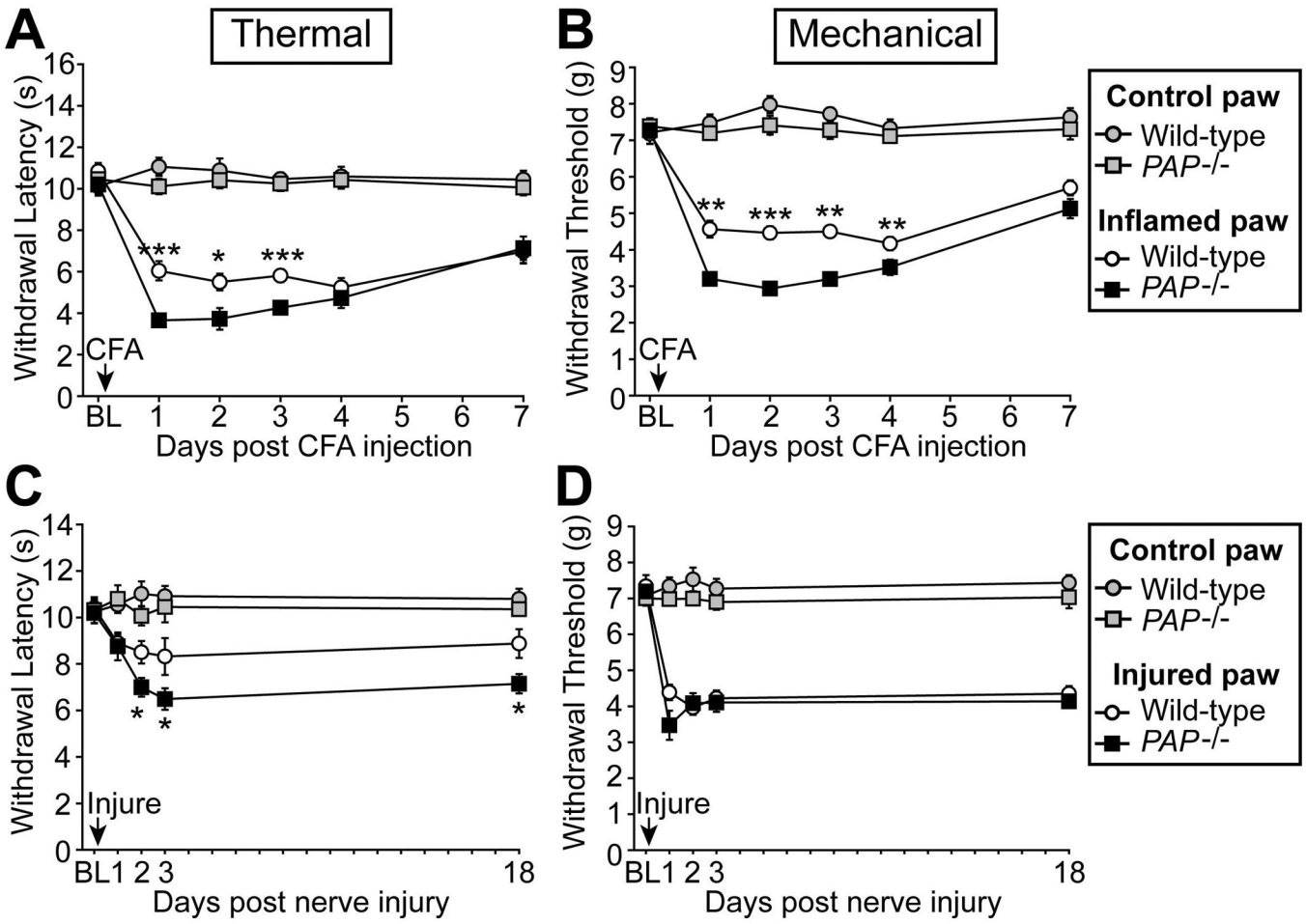

Figure 4. *PAP*$^{-/-}$ mice show enhanced nociceptive responses following inflammation and nerve injury

(A, B) CFA inflammatory pain model. Wild-type and *PAP*$^{-/-}$ mice were tested for (A) thermal sensitivity using a radiant heat source and (B) mechanical sensitivity using an electronic von Frey semi-flexible tip before (baseline, BL) and following injection of CFA (CFA-arrow) into one hindpaw. The non-inflamed hindpaw served as control. (C, D) SNI neuropathic pain model. The sural and common peroneal branches of the sciatic nerve were ligated then transected (Injure-arrow). Injured and non-injured (control) hindpaws were tested for (C) thermal and (D) mechanical sensitivity. (A–D) Paired t-tests were used to compare responses at each time point between wild-type (n=10) and *PAP*$^{-/-}$ mice (n=10); same paw comparisons. * $P < 0.05$; ** $P < 0.005$; *** $P < 0.0005$. All data are presented as means ± s.e.m.

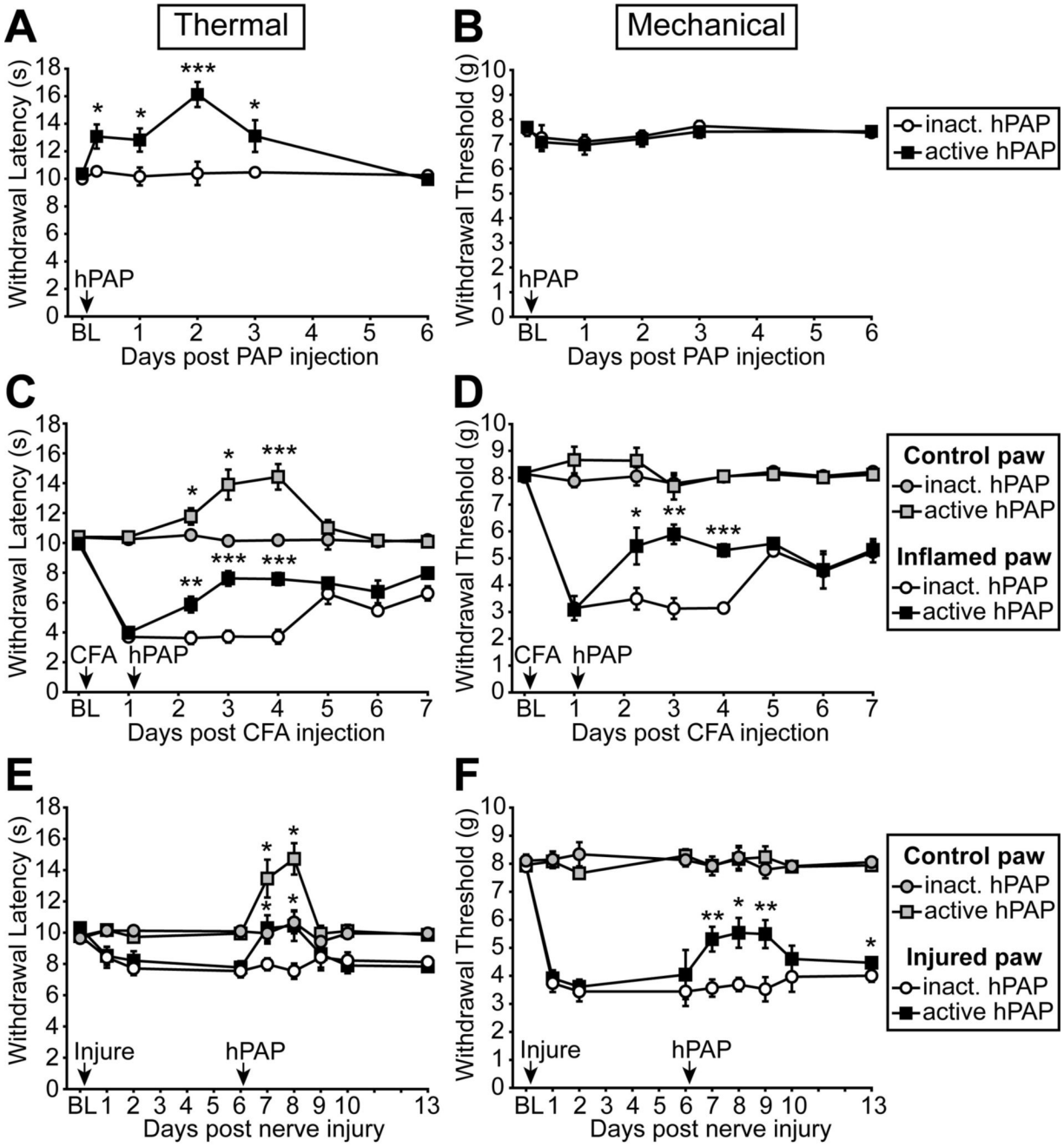

Figure 5. hPAP protein has long-lasting anti-nociceptive effects when injected intraspinally

(A, B) Wild-type mice were tested for (A) thermal and (B) mechanical sensitivity before (baseline, BL) and following i.t. injection of active or inactive hPAP (hPAP-arrow). (C, D) CFA inflammatory pain model. CFA was injected into one hindpaw (CFA-arrow). Active or inactive hPAP was i.t. injected one day later (hPAP-arrow). Inflamed and non-inflamed (control) hindpaws were tested for (C) thermal and (D) mechanical sensitivity. (E, F) SNI neuropathic pain model. The sural and common peroneal branches of the sciatic nerve were ligated then transected (Injure-arrow). Active or inactive hPAP was i.t. injected six days later (hPAP-arrow). Injured and non-injured (control) hindpaws were tested for (E) thermal and (F) mechanical sensitivity. (A–F) 250 mU hPAP injected per mouse. Paired t-tests were used to

compare responses at each time point between mice injected with active hPAP (n=10 mice per experiment) to mice injected with heat-inactivated hPAP (n=10 mice per experiment); same paw comparisons. * $P < 0.05$; ** $P < 0.005$; *** $P < 0.0005$. All data are presented as means ± s.e.m.

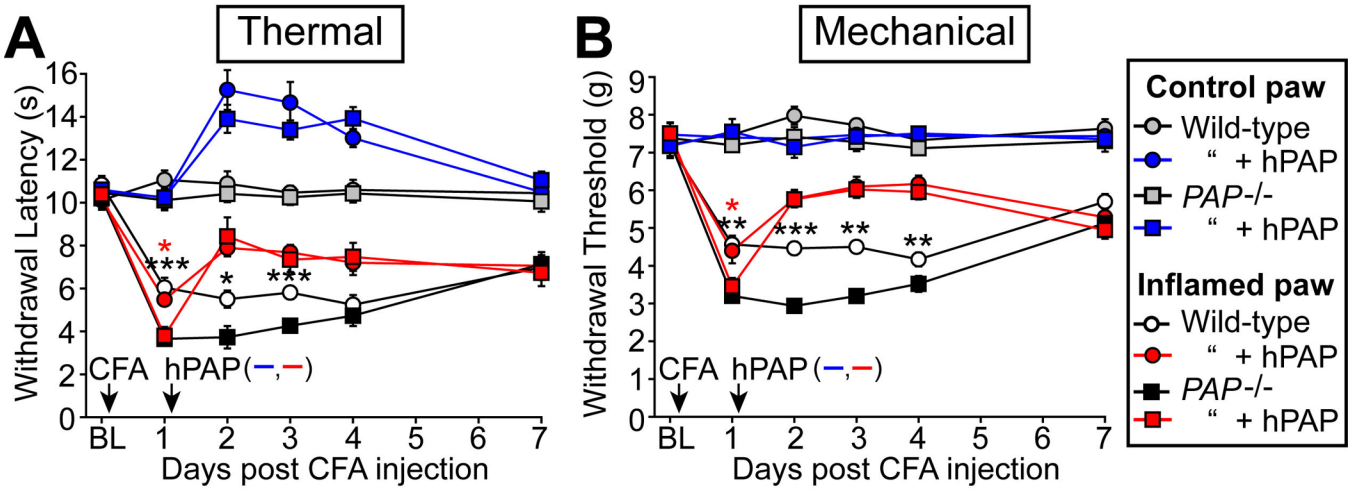

Figure 6. Intraspinal PAP has anti-nociceptive effects in *PAP*$^{-/-}$ mice and rescues the chronic inflammatory pain behavioral phenotype in *PAP*$^{-/-}$ mice

Wild-type and *PAP*$^{-/-}$ mice were tested for (A) thermal sensitivity and (B) mechanical sensitivity before (baseline, BL) and following injection of CFA (CFA-arrow) into one hindpaw. The non-inflamed hindpaw served as control. One day later, half of the wild-type and *PAP*$^{-/-}$ mice were injected with active hPAP (hPAP-arrow; 250 mU, i.t.; red and blue lines) while the other half were injected with inactive hPAP (black lines). Note: Data from these inactive hPAP injected mice were presented in Figure 4A, B. Paired t-tests were used to compare responses at each time point between wild-type (n=10/group) and *PAP*$^{-/-}$ mice (n=10/group); same paw comparisons (n=40 mice were used for this experiment). * $P < 0.05$; ** $P < 0.005$; *** $P < 0.0005$. All data are presented as means ± s.e.m.

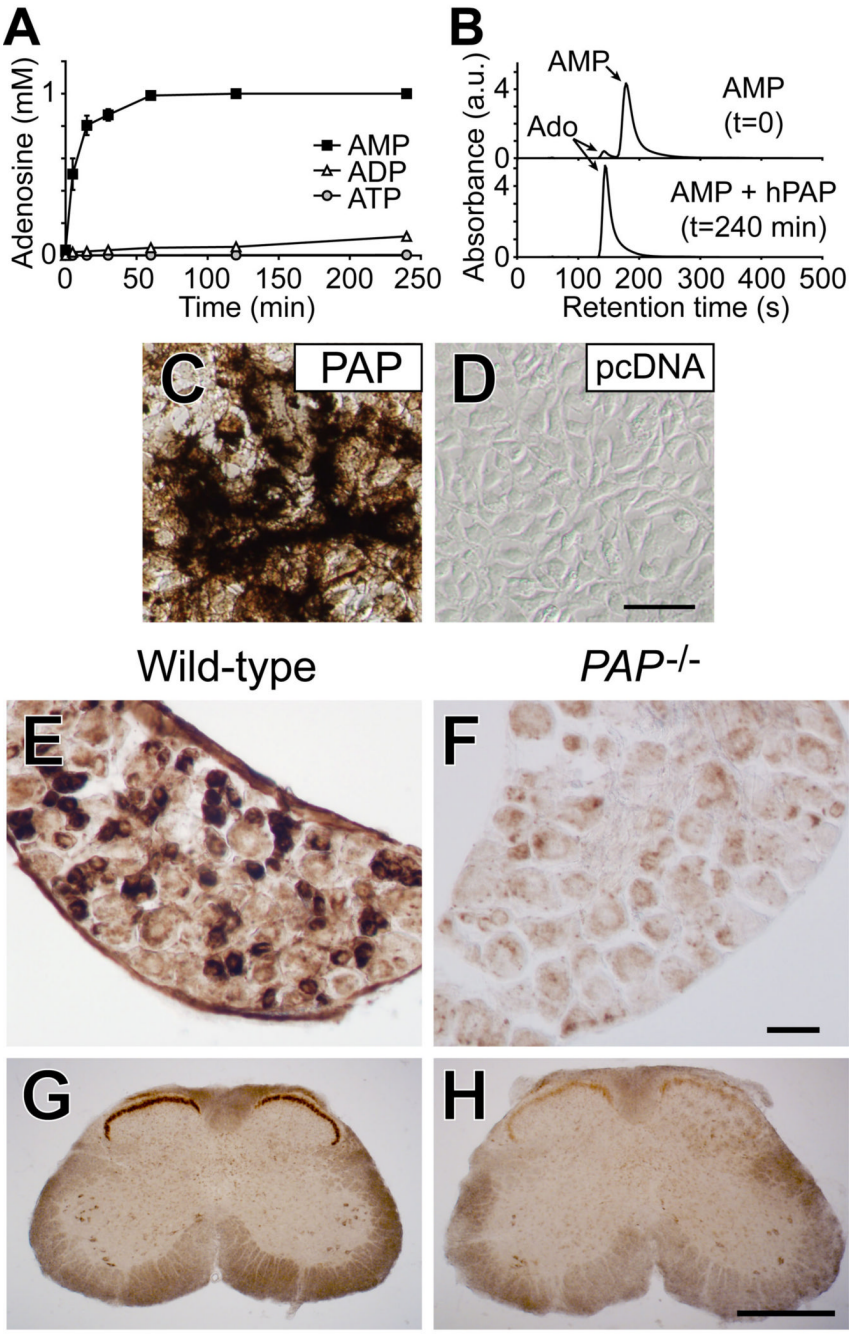

Figure 7. PAP has ecto-5'-nucleotidase activity as revealed by dephosphorylation of AMP to adenosine *in vitro*, in cells and in nociceptive circuits

(A) hPAP (2.5 U/mL) was incubated with 1 mM AMP, ADP, or ATP. Reactions (n=3 per time point) were stopped by heat denaturation at the indicated times. Conversion of nucleotides to adenosine was measured by HPLC. (B) HPLC chromatogram before (t=0) and after (t=240 min) incubation of 1 mM AMP with hPAP. Peaks corresponding to adenosine (ado) and AMP are indicated. Arbitrary units (a.u.). (C) HEK 293 cells were transfected with a mouse TM-PAP expression construct or (D) with empty pcDNA3.1 vector and then stained using AMP histochemistry. The plasma membrane was not permeabilized so that extracellular phosphatase activity could be assayed. (E–F) Lumbar DRG and (G–H) spinal cord from wild-type and

PAP$^{-/-}$ adult mice stained using AMP histochemistry. Motor neurons in the ventral horn of wild type and *PAP*$^{-/-}$ spinal cord were also stained. Identical results were obtained from five additional mice of each genotype. AMP (6 mM in C, D and 0.3 mM in E–H) was used as substrate and buffer pH was 5.6. Scale bar: 50 μm in C–F; 500 μm in G, H.

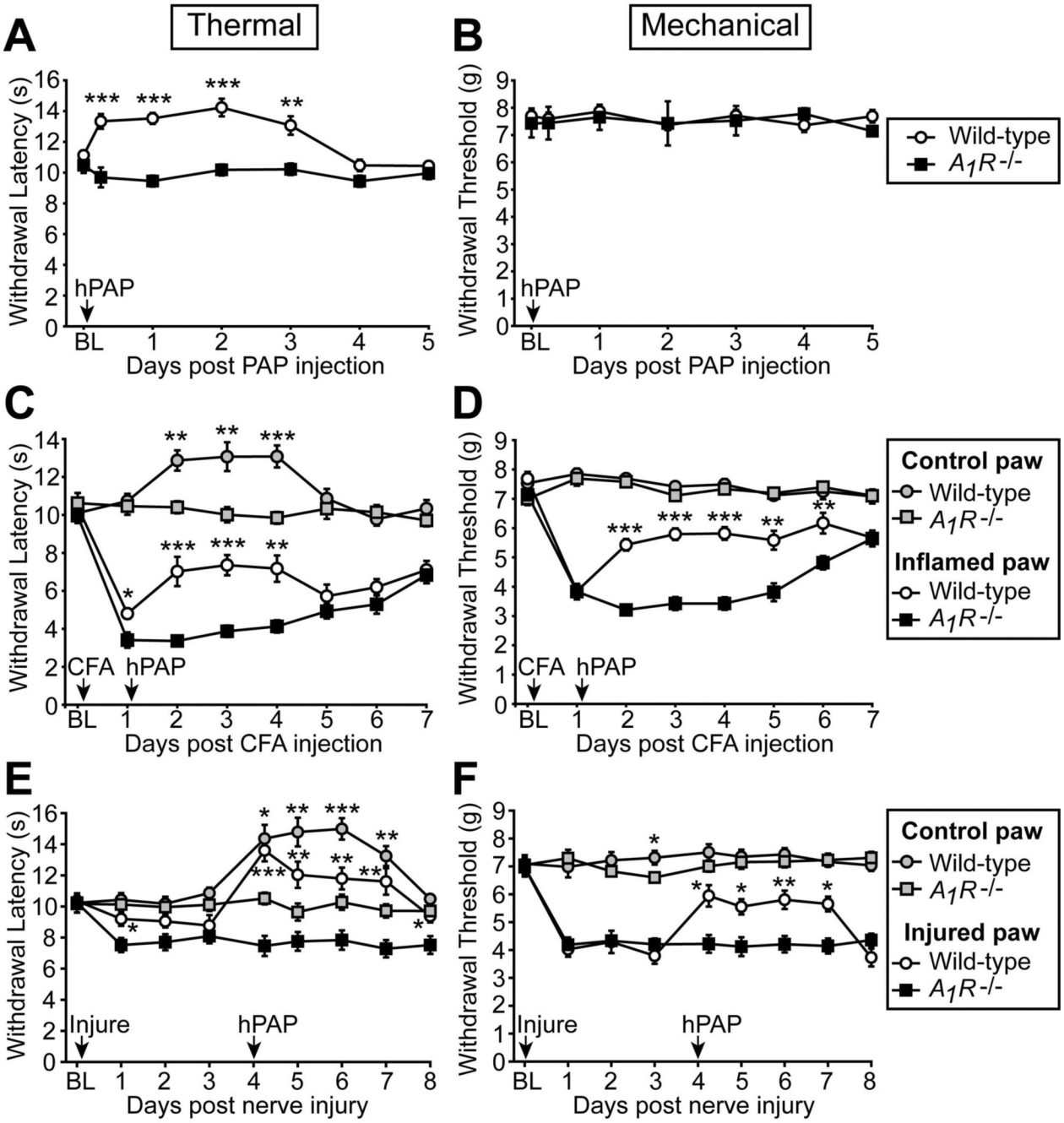

Figure 8. PAP requires A_1-adenosine receptors for anti-nociception

(A, B) Wild-type and $A_1R^{-/-}$ mice were tested for (A) thermal and (B) mechanical sensitivity before (baseline, BL) and following i.t. injection of hPAP (hPAP-arrow). (C, D) CFA was injected into one hindpaw (CFA-arrow) of wild-type and $A_1R^{-/-}$ mice. Active or inactive hPAP was i.t. injected one day later (hPAP-arrow). Inflamed and non-inflamed (control) hindpaws were tested for (C) thermal and (D) mechanical sensitivity. (E, F) The SNI model was used to induce neuropathic pain (Injure-arrow) in wild-type and $A_1R^{-/-}$ mice. Active or inactive hPAP was i.t. injected four days later (hPAP-arrow). Injured and non-injured (control) hindpaws were tested for (E) thermal and (F) mechanical sensitivity. For all experiments, 250 mU hPAP was injected per mouse. T-tests were used to compare responses at each time point between wild-

type (n=10) and $A_1R^{-/-}$ mice (n=9); same paw comparisons. * $P < 0.05$; ** $P < 0.005$; *** $P < 0.0005$. All data are presented as means ± s.e.m.